`Pendent_Drop`

Measuring liquid surface tension through the pendent drop method: description of a measurement bench and an ImageJ Plugin

Adrian Daerr* Adrien Mogne

Matière et Systèmes Complexes UMR 7057, Université Paris Diderot, 75205 Paris cedex 13, France

The pendent drop method for surface tension measurement consists in analysing the shape of an axisymmetric drop hanging from a capillary tube (Fig. 1). This article describes the principle and some practical considerations in implementing this method, both experimentally and numerically. Our numerical tool to match a theoretical profile to the contour of a pendent drop, either interactively or automatically, is available as an open-source `Pendent_Drop` Plugin for ImageJ [1]. This Plugin provides an estimate of the surface tension and other drop characteristics such as volume and surface area from the best matching parameters. We also present static and dynamic surface tension measurements on various liquids and a biosurfactant solution showing that this Plugin calculates values in accordance with known surface tensions and with those obtained via a commercial apparatus.

1. Introduction

The pendent drop method is commonly used to measure surface tensions of liquids. It consists in analysing the shape of a drop hanging typically from a capillary tube and about to detach. The method can also be applied to drops resting on a flat surface. For transparent liquids and in order to minimise interface contamination by adsorption from the gas phase, one can also work with bubbles, again either sessile or detaching from a tube. The shape of large drops or bubbles results from a competition between gravity, which tends to lengthen hanging drops or flatten sessile drops, and cohesive forces among liquid molecules which tend to produce compact, spherical drops. As

*adrian.daerr@univ-paris-diderot.fr

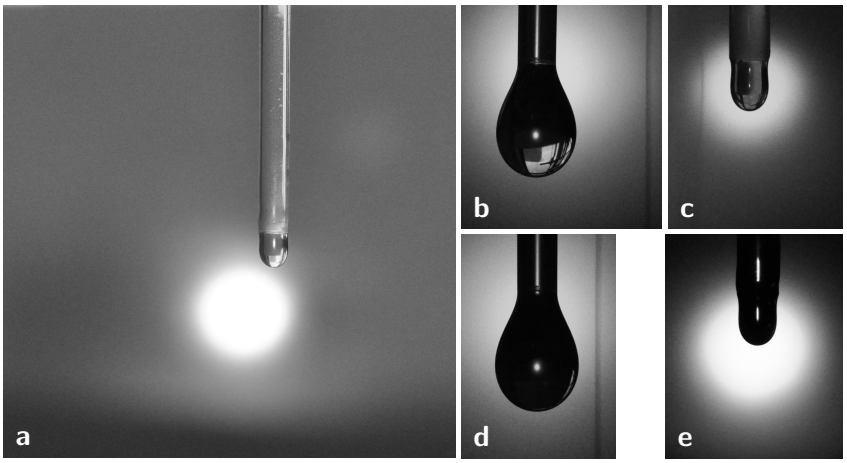

Figure 1: (**a**) Experimental set-up for pendent drop surface tension measurement: a drop is hanging from a capillary tube (diameter here: 1.68 mm). A light source far behind the drop provides a bright background against which the drop is photographed. (**b,c**) Drops of water and perfluorated oil close to the maximum volume before drop detachment. It is easy to see that the difference in surface tension has a tremendous effect on the drop shape. The pendent drop method consists in exploiting this strong dependency in order to determine an unknown surface tension. (**d,e**) After improving experimental conditions to get rid of spurious reflections and to enhance contrast.

shown in section 4, the resulting drop profile is described by only one non-dimensional parameter (tip radius over capillary length), although in practice five parameters have to be adjusted on a given image of a drop to account for unkown translation, rotation, scale and drop volume. In the Plugin presented here for example, the five parameters are the tip position and curvature, the tilt of symmetry axis and the capillary length. The profile determined this way gives access, besides to the surface tension, to other drop properties such as volume or surface area.

While both the theory and the set-up are rather simple and straightforward, to get precise, reliable and trustworthy results requires some care in experimental details. Note for example that surface tension depends quadratically on the capillary length, so that any error in the length measurements will result in twice that relative error on the surface tension:

$$\gamma = \rho g \ell^2 \qquad \Rightarrow \qquad \frac{\Delta\gamma}{\gamma} = 2\frac{\Delta\ell}{\ell}$$

The pendent drop technique is well established and there are numerous high quality commercial devices to measure not only static, but also dynamic properties of interfaces. These are however often available only in laboratories specialised in interface physics and chemistry. Here we show that within a few hours and with readily available and cheap material, high quality measurements can be achieved. This is not only useful to the biologist, geologist or environmental scientist who stumbles onto a case where surface

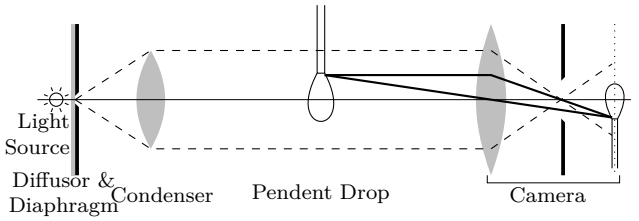

Figure 2: Schematics of a simple surface tension measurement set-up. The horizontal distances are much larger than depicted, both the light source and the camera being at about 30 cm from the drop, while the condenser lens has a diameter of 25 mm. We use a commercial DSLR camera with a Zeiss 50 mm Macroplanar objective, and a light emitting diode as a light source.

tension is a crucial parameter, but also enables college or high school teachers to explore the fascinating physico-chemistry of interfaces and surfactants (an example of surfactant adsorption dynamics is presented below).

As a rough rule, if a 2 %–5 % uncertainty on the surface tension is acceptable, a very simple set-up using a web-cam and a light source a metre away should be sufficient. This article describes a slightly more involved optical set-up using parallel light and a macro objective, and underlines the pitfalls that must be avoided in order to get a result that should be well within about 1 % of the true value. As always in metrology the experimental difficulty increases very quickly with the desired precision, as more and more small physical phenomena start having a noticeable effect on the measurement. Relative uncertainties of and below 10^{-3} are beyond the scope of this article, requiring an improved set-up with a telecentric objective and much better control of the atmosphere, temperature, vapour pressure, vibrations *et cætera* than was attempted by the authors.

The structure of this article is as follows: the two following sections 2 and 3 describe the measurement bench and present data measured with the Plugin in comparison to reference data. Sections 4 and 5 describe the underlying theoretical framework and the plugin's inner architecture, respectively. Appendix A summarises the properties that the input image must have for the Plugin to give meaningful results, and the appendices B and C contain usage and installation instructions for the `Pendent_Drop` surface tension measurement Plugin for ImageJ.

2. Measurement bench

Our measurement set-up is depicted in fig. 2. The condenser is at its focal length from the light source diaphragm, so that light rays are parallel to the optical axis in the limit of a closed diaphragm. The camera is focalised on the drop. The drop is extruded either from a Pasteur pipette, or from a micropipette plastic tip. The pipette is connected to a syringe that is driven either by hand or by a syringe pump.

This basic measurement bench is quite easy to set up. It can even be simplified further by replacing the light source and condenser by a bright screen at a large distance from

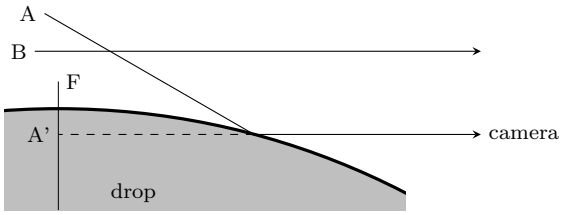

Figure 3: Light reaching the drop from direction A will be partially reflected towards the camera, whose focal plane cuts through the drop at F. The light will appear as coming from point A', and be almost as bright as direct light from e.g. B, because the reflection coefficient tends to unity for near grazing incidence. As a result, the drop may appear slimmer than it is.

the drop. In any case the drop appears dark against a light background, because even for transparent liquids light rays traversing the drop will be refracted at the interface and miss the camera entrance pupil (except at the very center of the drop, where a small image of the light source can be seen because the interfaces are perpendicular to the optical axis).

Despite the simplicity of the set-up is important however to be aware of a few effects that can affect the measurement quality. The drop can indeed appear smaller than its real size for several reasons. One consists in grazing reflections at the border of the drop (fig. 3). For incident angles above about 82° on water for example, the reflected intensity lies above 50 % of the incident intensity, so that the corresponding points on the drop will be classified as outside. This corresponds to an error on the drop radius of about 1 %, and therefore an error on the surface tension of 2 %. Note that the error on the surface tension is most likely even larger, because eroding the drop image by a few pixels does not amount to a mere change in scale: the drop's vertical extent is usually larger than its horizontal diameter, so that eroding sides and bottom by the same amount of pixels will change its aspect ratio and lead to an unphysical profile that cannot even be accurately adjusted by the Young-Laplace equation any more.

The condenser set-up prevents this source of errors by providing only near-parallel light rays. Alternatively this selection of light parallel to the optical axis can also be achieved by a telecentric lens on the camera side, as this type of lens is precisely built to have its aperture stop virtually infinitely far from the imaged object. Using a telecentric lens comes with the added benefit of having a magnification which is independent of the drop's distance to the camera, thereby reducing potential errors when calibrating the image scale. The commercial apparatus against which we validate our measurement bench and numerical analysis (see next section) uses such a telecentric lens, and a simple back-lit ground glass as an extended omnidirectional light source.

Errors also arise from oversaturating the image sensor, for two reasons. One is that common CCD and CMOS sensors present some degree of blooming, meaning that electrons from oversaturated pixel wells overflow into adjacent pixels and/or fail to completely transfer (mainly in the case of CCDs) during pixel read-out, causing neighbouring

	water	hexadecane	mercury
Temperature	303 K	303 K	295 K
Density	995.7 kg/m^3[7]	767.7 kg/m^3[8]	13 541 kg/m^3[7]
capillary length ...			
from literature	2.70 mm[7]	1.885 mm[9]	1.89 mm (293 K)[7]
imaging and analysis:	2.703 mm	1.863 mm	1.70 mm
our set-up and sofware	±0.015 mm	±0.018 mm	±0.015 mm
imaging and analysis:	2.697 mm	1.882 mm	—
commercial apparatus	±0.01 mm	±0.02 mm	
imaging: com. apparatus	2.750 mm	1.890 mm	—
analysis: our software	±0.01 mm	±0.03 mm	

Table 1: Comparison of capillary lengths of three liquids from different sources.

pixels (*viz* pixels in the same column) to appear much brighter than they should. The second reason is that our Plugin puts the drop interface at half the intensity contrast between drop and background. If the background intensity is oversaturated and the captured picture therefore presents intensities clipped to values below a maximum, the 50 % threshold on the (clipped) pixel values amounts to a lower threshold on the real intensity interval, again effectively shifting the drop contour inwards. To prevent these effects the background illumination must be as uniform as possible, and the camera aperture and exposure time chosen so as not to saturate the sensor.

3. Validation measurements

The following table compares capillary length measurements for three liquids (water, hexadecane and mercury) using our set-up and sofware with values from the literature and values measured using a commercial apparatus (Teclis Instruments: Tracker, software version 9.7.0). Additionally, we report the capillary length that our software determines from images taken on the commercial apparatus. In all cases the indicated uncertainty is the standard deviation of three to twelve drops, each measured two to four times (varying lighthing, exposure settings and the part of the drop to which the theoretical contour was adjusted). Mercury vapour represents a health hazard, and its vapour pressure depends strongly on the temperature[6]. Considering the high summer temperatures of around 30 °C, we refrained from performing measurement of mercury drops using the commercial apparatus which could not easily be relocated. We could however transfer our bench to an air-conditioned room to perform the measurement on mercury at about half the vapour pressure.

Our measurements for water and hexadecane agree with literature values as well with

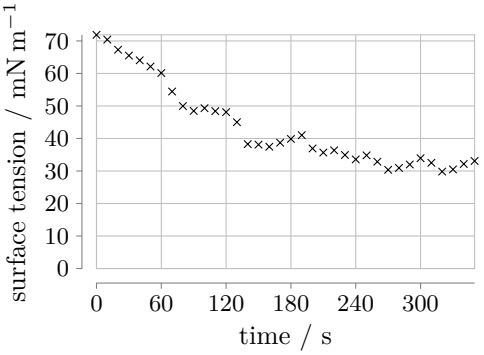

Figure 4: Surface tension of a drop of surfactine solution over time.

the values obtained through the commercial apparatus. The measurements for mercury yield a capillary length about 10 % lower than expected. We suspect that oxidation of its surface in air may have been responsible for lowering the surface tension. Analysing the images from the commercial apparatus with our software slightly overestimates the capillary length of water, possibly to a small error on the independently performed image scale calibration. In any case, all measurements for water and hexadecane differ by less than 1 %, giving a conservative estimate of the precision of our set-up and analysis.

3.1. Example of slow surfactant dynamics

If the surface tension varies over time, the measurement of the surface tension on successive images can be performed efficiently by taking each result of a fit as a starting guess for the adjustment of the following image, which is what the `Pendent_Drop` Plugin will do automatically if run on a stack. Fig. 4 shows the time evolution of the capillary length and surface tension of an acqueous solution of surfactine, a lipopeptidic bio-surfactant (molecular weight 10^3 Da) produced by the bacteria *B. subtilis*. When the drop is initially extruded from the capillary, fresh interface is created that is only weakly populated with surfactant molecules, so that the surface tension is close to that of pure water. Over time surfactant molecules diffusing in the liquid reach the free surface and adsorb to the interface. It takes several minutes for the molecule concentration at the interface to reach an equilibrium.

The irregular decrease of the surface tension, especially the sudden drops around $t = 70\,\mathrm{s}$ and $t = 130\,\mathrm{s}$ are not due to measurement errors, but to variations of the drop volume by the human operator. Recall that for a reliable surface tension measurement the curvature must vary significantly from top to bottom, therefore the drop size needs to be of the order of the capillary length. However the drop is then also close to pinch-off because the maximum drop size before pinch-off is of the order of $(d\ell_c^2)^{1/3}$ where d is the tube diameter. As the surface tension, and thus ℓ_c, decreases over time in the case of the surfactine drop, the drop volume has to be diminished to prevent pinch-off, by pulling liquid back into the capillary tube before the drop becomes unstable. This

reduces the free surface and increases the surface density of surfactant molecules, which in turn results in a further decrease of the surface tension. On the other hand, if the drop volume is increased as around $t = 180\,\mathrm{s}$, the drop surface also increases and the surfactant is diluted at the interface, increasing the surface tension. In order to measure the change in surface tension excusively due to adsorption of new surfactant molecules, a feedback loop is needed that maintains a constant drop surface.

4. Physics of the pendent drop

Cohesive forces between the molecules of the liquid prevent the pendent drop from detaching under its weight, up to a critical size. The effect of these cohesive forces is thermodynamically described by a contribution $\gamma\,\mathrm{d}S$ to the free energy that is proportional to the surface variation $\mathrm{d}S$, where γ is the surface free energy or surface tension. In other words, cohesion is accounted for by considering that the free surface of a liquid is under tension, and the equilibrium shape is one minimising this surface together with the potential energy.

To establish an equation describing the shape of an axisymmetric pendent drop (fig. 5), it is easier to consider the local pressure balance. Just like the pressure inside of a rubber balloon is higher than outside, surface tension is responsible for a pressure jump across a curved interface, that is related to its mean curvature $\bar{\kappa}$ by Young-Laplace's formula $\Delta p(z) = \gamma\bar{\kappa}(z)$.

Now in a pendent drop the pressure jump across the interface varies with height, because of the density difference between the inner liquid and outer gas phase, implying that the surface curvature must vary as well. Indeed, the drop has an equilibrium shape if and only if the hydrostatic pressure difference is everywhere equal to the Young-Laplace pressure jump across the interface.

Take the lowest point of the drop as origin for the height coordinate z. Then the pressure inside the drop is $p_{\mathrm{in}}(z = 0) - \rho_{\mathrm{in}}gz$ at a distance z above it, while it is $p_{\mathrm{out}}(z = 0) - \rho_{\mathrm{out}}gz$ outside at the same height. g denotes gravitational acceleration and $\rho_{\mathrm{in/out}}$ the densities of the respective phases. Noting $\Delta p_0 = p_{\mathrm{in}}(z = 0) - p_{\mathrm{out}}(z = 0)$ the pressure drop at the drop tip, and $\Delta\rho = \rho_{\mathrm{in}} - \rho_{\mathrm{out}}$ the density contrast, we have a pressure jump across the interface $\Delta p(z) = \Delta p_0 - \Delta\rho gz$ at height z. Note that the value of Δp_0 is unkown beforehand. It depends on the geometry of our set-up and the drop volume, and constitutes an integration constant.

At equilibrium, this hydrostatic pressure jump is equal to the Laplace pressure given above: $\Delta p_0 - \Delta\rho gz = \gamma\bar{\kappa}(z)$. We parametrise the drop surface in cylindrical coordinates as $(R(s), Z(s))$, where s is the curvilinear distance to the tip along the interface. Expressing the mean curvature as a function of R, Z and the angle ψ between the tangent plane to the interface and the horizontal: $\mathrm{d}R/\mathrm{d}s = \cos\psi$, one obtains the following expression for the pressure equilibrium:

$$-\frac{1}{\ell_c^2}\sin\psi = \frac{\mathrm{d}}{\mathrm{d}s}\left(\frac{\mathrm{d}\psi}{\mathrm{d}s} + \frac{\sin\psi}{R}\right).$$

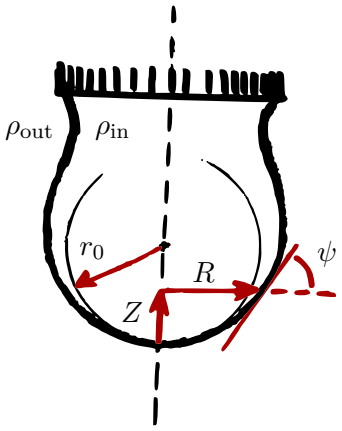

Figure 5: Notations. The drop profile is assumed to be axisymmetric, and is described by the two cylindrical coordinates $R(s)$ and $Z(s)$ as a function of the curvilinear parameter s. The local tilt ψ with respect to the axis normal enters the expression for the interface curvature, and is related to R through $R' = \cos\psi$. We have spherical symmetry at the very tip, with radius r_0.

The boundary conditions at the drop tip are $\psi(0) = 0$ and $\mathrm{d}\psi/\mathrm{d}s = p(0)/2\gamma = 1/r_0 =$ const., where r_0 is the radius of curvature of the drop tip which has locally spherical symmetry. Scaling all lengths by the characteristic length $\ell_c = \sqrt{\gamma/\Delta\rho g}$ (called *capillary length*) yields one universal drop shape equation

$$-\sin\psi = \frac{\mathrm{d}}{\mathrm{d}s}\left(\frac{\mathrm{d}\psi}{\mathrm{d}s} + \frac{\sin\psi}{R}\right) \qquad \text{with } \psi(0) = 0 \text{ and } \psi'(0) = \ell_c/r_0, \tag{1}$$

Note that the solutions (i.e. all possible axisymmetric drop shapes) are fully determined by the choice of the initial condition for $\psi'(0)$, which is just the ratio of the capillary length and the radius of curvature of the drop tip.

5. What the Plugin does internally

numérical integration

The equation (1) is integrated for a given parameter $\ell_c/r_0 = 1/r_*$ using a fourth order Runge-Kutta scheme. Near the drop tip the integral equation becomes singular as $R \to 0$, but the solution itself is perfectly regular: it is simply a nearly perfectly spherical profile (at least at distances small with respect to capillary length and tip radius). We can thus use an analytical solution to get away from the singularity at $R = 0$. The leading order terms of that solution are

$$\left.\begin{array}{rcl} R &=& r_* \sin\frac{s}{r_*} + \frac{s^5}{40r_*^2} + O(s^6) \\ Z &=& \frac{1}{2r_*}s^2(1 + (\frac{1}{16} - \frac{1}{12r_*^2})s^2) + O(s^6) \\ \psi &=& s/r_*(1 - s^2/8) + O(s^5) \end{array}\right\} \text{for} \quad s \ll 1 \wedge s \ll r_*$$

We use this solution to calculate the first piece of drop contour where $s \ll 1$ and $s \ll r_*$. Then we continue through numerical integration.

matching the theoretical solution to the image of the drop

The drop contour from the previous integration is then rescaled, translated and rotated according to the given parameters (tip position, curvature, and gravity angle) to be

compared to the experimental drop image. A distance between this theoretical contour $\mathcal{C}$ and the observed drop border $\mathcal{B}$, is then calculated as the sum, over all pixel rows and both sides of the drop, of the difference of horizontal positions:

$$\chi^2 = \sum_z |x_{\mathcal{C},\text{left}}(z) - x_{\mathcal{B},\text{left}}(z)|^2 + |x_{\mathcal{C},\text{right}}(z) - x_{\mathcal{B},\text{right}}(z)|^2$$

The drop border $\mathcal{B}$ is detected beforehand by matching a step-function to the image intensity profile in a neighbourhood of the interface.

optimize by varying parameters and iterating
In case automated fitting of some parameters is requested (by pressing the "fit" or the "OK" button), the Plugin tries to minimise the distance function χ^2 using an algorithm by Powell [4, 5]. This algorithm consists in successively varying each parameter, searching for each the value that will yield the best-fitting integrated drop contour. The user can choose which parameters are adjusted in this prodecure, and which ones are kept fixed. After all free parameters have been varied, the algorithm checks whether it is not more efficient to minimise along another direction in parameter space, i.e. modify several parameters concurrently, and possibly updates the list of directions. The whole process is repeated until the change in the fit distance χ^2 after a full round becomes too small.

A. Prerequisites

The Plugin is run on a high contrast image of a pendent drop (Fig. 6-left). Pixel values are expected to be close to zero within the drop, and close to saturation (i.e. 255 for 8-bit images) outside. This is typically obtained by taking the picture of the drop in front of a light background far away from the drop (Fig. 1). Bright spots well within the drop are not a problem, but contrast should be good in the vicinity of the contour. Note however that saturation should be avoided at all cost, both because of blooming effects in the light sensitive image recording device and because it tends to bias the interface detection towards the inside of the drop. See also section 2.

B. Pendent_Drop ImageJ Plugin Usage

By default, the `Pendent_Drop` Plugin appears in the Plugins menu of ImageJ, in a folder termed `Drop Analysis`. The menu item `About Pendent Drop` will show a bit of information on the Plugin, including usage, the update site and an example image on which you can test the Plugin. The menu item `Pendent Drop` launches the Plugin itself.

Draw a rectangular Region Of Interest (ROI) around the pendent drop before calling the Plugin (Fig. 6-middle). The ROI should not include the inlet tube, but only the free surface of the drop. A few ten or so pixels margin around the drop is sufficient for the interface detection to perform correctly.

Fill in any parameter values you know, and check the plausibility of the initial guess for the others. If the image was calibrated for spatial scale, the corresponding scale is

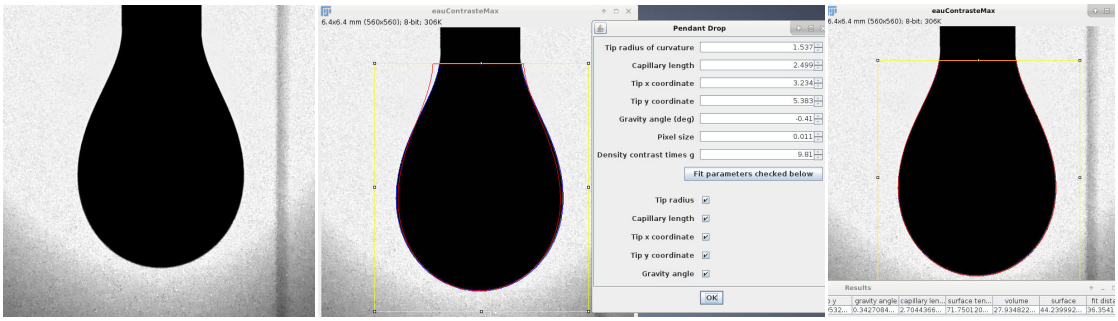

Figure 6: Plugin usage. **(left)** starting image, contrasted just short of saturating black and white levels. **(middle)** image with rectangular ROI selection and initial guess next to Plugin dialog. **(right)** The profile after automatic optimisation of the parameters.

proposed by the Plugin and all length scales are expressed in calibrated units. If the image is not calibrated all lengths are given in pixels, including the resulting capillary length. The angle specifies the tilt of the symmetry axis away from the vertical, in degrees.

Two overlays are shown on the image: a blue line indicating the drop border as detected by the Plugin, and a red line representing the profile described by the current parameter values.

a) modify the parameters so as to improve the visual accordance of theoretical profile and image. In version 2.0.0 of the Plugin a measure of the distance between profile and border is logged to the console, it should be made as small as possible.

b) check those parameters that the Plugin may adjust and click on the button for automatic minimisation. Only the previously checked parameters are varied when trying to find an optimal shape. The overlay is updated accordingly. Note that the minimisation algorithm can get trapped in a local minimum, so try starting from different initial values and compare the results. Also check whether the resulting profile looks satisfactory.

Clicking the `OK` button will cause the Plugin to fit each slice of the active stack by a drop profile. The dialog parameters serve as starting point for the fit of the first slice, while subsequent slices are adjusted starting from the result of the previous slice. The resulting drop shape descriptors, surface tension and drop properties (volume, surface) for each slice are summarised in a result table.

How to get the surface tension If the image was scale-calibrated, and a sensible value was entered for the '`density contrast times g`' parameter (the difference of the densities in/outside the drop multiplied by your planet's gravitational acceleration, $(\rho_{\text{in}} - \rho_{\text{out}})g = \Delta\rho\, g$), then the surface tension is indicated in physical units. For example if the `pixel size` is in millimetres per pixel, and the `density contrast times g` is in grams per square second and square millimetre (e.g. around $9.8\,\text{g}\,\text{mm}^{-2}\,\text{s}^{-2}$ for water in air on earth), then the indicated surface tension is in $\text{g}\,\text{s}^{-2}$ or milli-Newton per metre. Otherwise the unit conversion has to be performed by hand. Recall that surface tension

γ is calculated from the capillary length using the formula $\gamma = \Delta\rho g \ell_c^2$.

C. Installing the Pendent_Drop Plugin for ImageJ

via the update site The preferred method is to use Fiji's [2, 3] update mechanism. Detailed step-by-step instructions with illustrations can be found at `http://fiji.sc/How_to_follow_a_3rd_party_update_site`. This software is hosted at `http://fiji.sc/List_of_update_sites`.

In the `Help` menu, select `Update Fiji` to start the updater. Choose the `Advanced mode`, click on `Manage update sites` and add a site with the following URL:

`http://sites.imagej.net/Daerr/`

(The name has no particular importance, choose something meaningful to you)

Enable this site (check the box next to it) and close the window to get back to the main updater window. In the list of Plugins, locate `plugins:pendent_drop-2.0.0.jar` (to find it more easily you can restrict the list to items from the new site using the menu above the list), select it and mark it for installation. Apply changes, restart Fiji: a new folder `Drop Analysis` should appear in the Plugins menu.

by downloading the jar file For a manual installation, and as usual with ImageJ Plugins, just put the jar into ImageJ's `plugins` folder or a subfolder thereof. Restart ImageJ to see the Plugin.

by building from the source The source code of the `Pendent_Drop` Plugin is hosted on gitlab at `https://github.com/adaerr/pendent-drop`. You will need tools such as `git` and a java compiler and be familiar with their usage. If you are using `maven`, then the command `mvn package` should produce a jar file for you in the `target` directory. Check the git history to identify usable states that you can check out and compile.

References

[1] W. S. Rasband, *ImageJ*, U. S. National Institutes of Health, Bethesda, Maryland, USA, `http://imagej.nih.gov/ij/`, 1997-2010.

[2] Fiji web site: `http://fiji.sc/`

[3] J. Schindelin *et al.*, *Fiji: an open-source platform for biological-image analysis*, Nature Methods 9(7), pp.676–682 (2012)

[4] M. J. D. Powell, *Computer Journal* **7** (1965) 155

[5] S. Brandt, *Datenanalyse*, BI-Wiss.-Verlag (Mannheim, Leipzig, Wien, Zürich) 3rd edition, ISBN 3-411-03200-6 (1992)

[6] F. M. Ernsberger and H. W. Pitman, *New absolute manometer for vapor pressures*, Rev. Sci. Instrum. **26**(6): 584–589; 1955. M. L. Huber, A. Laesecke and D. G. Friend, *The vapor pressure of Mercury*, NISTIR report 6643 (2006), URL: `http://www.boulder.nist.gov/div838/SelectedPubs/NISTIR.6643.pdf`

[7] D'Ans and Lax, *Taschenbuch für Chemiker und Physiker*, Springer, 1967 (3rd edition), pp. 1-134f, 1-600ff, 1-607, 1-901

[8] S. S. Joshi, *Thermodynamic Interactions in Mixtures of Bromoform with Hydrocarbons*, J. Phys. Chem. **95** (1991) 5299–5308

[9] L. I. Rolo, A. I. Caço, A. J. Queimada, I. M. Marrucho, and J. A. P. Coutinho, *Surface tension of Heptane, Decane, Hexadecane, Eicosane and Some of Their Bianary Mixtures* J. Chem. Eng. Data **47** (2002), 1442–1445